

Suppression and Control of Pre-thermalization in Multi-component Fermi Gases Following a Quantum Quench

Chen-How Huang,¹ Yosuke Takasu,² Yoshiro Takahashi,² and Miguel A. Cazalilla^{1,3,4}

¹*Department of Physics, National Tsing Hua University, Hsinchu 30013, Taiwan*

²*Department of Physics, Graduate School of Science, Kyoto University, Kyoto 606-8502, Japan*

³*National Center for Theoretical Sciences (NCTS), Hsinchu City, Taiwan*

⁴*Donostia International Physics Center (DIPC), Manuel de Lardizabal, 4 San Sebastian, Spain*

(Dated: October 23, 2019)

We investigate the mechanisms of control and suppression of pre-thermalization in N -component alkaline earth gases. To this end, we compute the short-time dynamics of the instantaneous momentum distribution and the relative population for different initial conditions after an interaction quench, accounting for the effect of initial interactions. We find that switching on an interaction that breaks the $SU(N)$ symmetry of the initial Hamiltonian, thus allowing for the occurrence of spin-changing collisions, does not necessarily lead to a suppression of pre-thermalization. However, the suppression will be most effective in the presence of $SU(N)$ -breaking interactions provided the number of components $N \geq 4$ and the initial state contains a population imbalance that breaks the $SU(N)$ symmetry. We also find the conditions on the imbalance initial state that allow for a pre-thermal state to be stabilized for a certain time. Our study highlights the important role played by the initial state in the pre-thermalization dynamics of multicomponent Fermi gases. It also demonstrates that alkaline-earth Fermi gases provide an interesting playground for the study and control of pre-thermalization.

I. INTRODUCTION

Dilute Fermi gases of alkaline-earth atoms (AEAs) like ^{173}Yb or ^{87}Sr exhibit a remarkable unitary symmetry at ultracold temperatures [1–3]. The latter is ultimately a consequence of their closed-shell (ground-state) electronic structure, 1S_0 : For AEAs, the atomic total angular momentum \mathbf{F} in their ground state equals the nuclear spin \mathbf{I} . Due to the weakness of hyperfine interactions, \mathbf{I} is essentially decoupled from the electronic degrees of freedom. Thus ultracold gases of AEAs can be viewed as spin- I particles interacting with a pseudo-potential that is independent of their nuclear spin orientation, I_z and therefore invariant under the larger unitary group $SU(N = 2I + 1)$. The accuracy of this $SU(N)$ -symmetric description of interaction has been confirmed experimentally [4, 5]

Recently, this property has attracted a great deal of interest in connection with the possibility of quantum emulation of $SU(N)$ -symmetric models of interest to condensed matter physicists [1, 2, 6–19]. In recent years, many experiments along this direction have been carried out [20–26] (See also [3] for a recent review). In addition, the realization of $SU(N > 2)$ symmetric many-body systems is relevant to the understanding of some aspects of the strong force that binds quarks into nucleons [27, 28]. Indeed, as a quantum emulator of $SU(N)$ interacting fermion gas for which N can be as large as 10, ultracold gases of AEAs can provide an ultracold realization of certain toy models of quantum chromodynamics (QCD) [28]. In this regard, it is interesting to explore any further connections between ultracold gases of AEAs and quark-gluon physics. Indeed, an idea that has recently emerged in the study of the quark-gluon plasma is the existence of *pre-thermalized* states [29]. The latter are

characterized by the rapid establishment of a kinetic temperature whilst, at the same time, the distribution of the eigenmodes of the system has not reached thermal equilibrium as described by the Fermi-Dirac or Bose-Einstein distributions. Pre-thermalized states have been extensively discussed in relation to the non-equilibrium dynamics of ultracold atomic gases [30–49]. In earlier work, it was also shown [32] that pre-thermalization can be also linked to the existence of an integrable truncated version of the Hamiltonian that describes the short-time dynamics [32] and can be related [32] to the non-thermal states occurring in integrable systems, which are described by the generalized Gibbs ensemble [42, 45, 46, 50–57]. However, for non-integrable systems, the system will eventually relax at long times to a thermal state described by a standard Gibbsian ensemble [58–66]. However, if the breaking of integrability is weak, the pre-thermalized state emerging at short times can be fairly long lived [30, 31, 34–41, 44, 45, 47, 48, 67–75].

Understanding the conditions under which a system exhibits pre-thermalization is an important ongoing research effort. In this work, we investigate the control and suppression of the pre-thermalized behavior by the choice of the initial state and the symmetries of the post-quench Hamiltonian. Mathematically, the emergent $SU(N = 2I + 1)$ symmetry described above forbids spin-changing collisions that change the relative population of the different spin components (cf. Fig. 1). Thus, we shall consider the short-time dynamics of an AEA Fermi gas following a sudden interaction quench in which the postquench Hamiltonian breaks the $SU(N)$ symmetry. We analyze under which conditions this system exhibits pre-thermalization and, in particular, how the latter is affected by allowing for spin-changing collisions. It is known [30–32, 39] that the existence of pre-thermalized

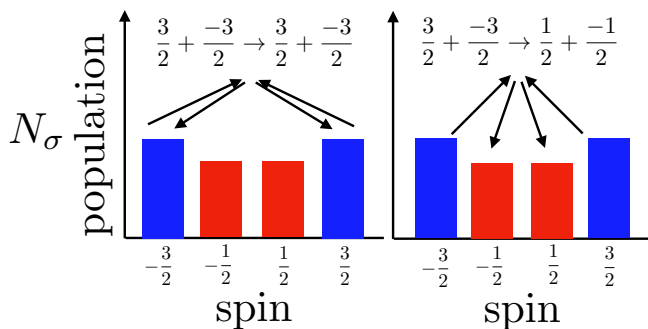


FIG. 1. Two possible scattering processes in an SU(4) Fermi gas following a quench of the interaction that breaks the emergent SU(4) symmetry, starting from an initial state with population imbalance. **Right panel:** Spin-changing collision (as understood in this work) defines a two-atom collision that modifies the relative spin populations. **Left panel:** Other scattering processes that conserve total spin and do not change the relative spin-population.

states in Fermi gases is related to the lack of phase space for inelastic collisions to redistribute the excitations that are created following the quench. Thus, thermalization is only possible after enough phase space has been created for inelastic collisions to efficiently take place [30, 31, 39]. The latter take place more efficiently as the strength of the quenched interaction is increased. This expectation has been confirmed numerically [67, 74]. In this work we further analyze this issue and show that the mere existence of phase space allowing for inelastic collisions in the initial state is a necessary but *not sufficient* condition for the suppression of pre-thermalization. Furthermore, the existence of matrix elements of the interaction allowing for inelastic collisions is not sufficient if it is not accompanied by the existence of phase space in the initial for the latter to take place. Nevertheless, as we show below, it is possible to find certain types of initial states for which the rate at which the inelastic collisions happens at intermediate times vanishes.

The rest of this article is organized as follows. The details of the model as well as the methods employed for the study of pre-thermalization are discussed in Sec. II. In Sec. A, the details of the calculations of the instantaneous momentum distribution are provided. In Sec. IV, we describe the quench dynamics in the two-component gas. In Sec. V we report the results for the four-component gas and discuss the effects of spin-changing collisions and the spin-imbalance in the initial state. In Sec. VII, we provide the conclusions of this work and summarize the main results. Some details of the calculations are given in Appendix A. Henceforth, we shall work in units where $\hbar = 1$.

II. MODEL AND METHODS

An interaction quench in an AEA ultracold gas can be described by means of the following Hamiltonian:

$$H(t) = H_0 + U_1(t), \quad (1)$$

$$H_0 = K + U_0, \quad (2)$$

$$K = \sum_{p\sigma} \epsilon_p c_{p\sigma}^\dagger c_{p\sigma}, \quad (3)$$

where $\epsilon_p = p^2/2m$ is the single-particle dispersion, and $c_{p\sigma}, c_{p\sigma}^\dagger$ are the annihilation/creation operators of fermions with momentum p and spin σ obeying $\{c_{p\alpha}, c_{k\beta}^\dagger\} = \delta_{\alpha,\beta} \delta_{p,k}$ (and anti-commuting otherwise); U_0 is the initial (SU(N)-symmetric [1–3]) interaction, and $U_1(t) = \theta(t)U_1$ is the quenched interaction (see below), $\theta(t)$ being Heaviside's step function, which describes a sudden quench of the interaction term U_1 . The generalization of our methods to other types of quenches has been presented in Ref. [76], where special attention was paid to the proper definition of the energy and the asymptotic behavior of the momentum distribution out of equilibrium. In the sudden quench limit, the calculation of dynamics of the total energy is less involved, see discussion at the end of this section.

In general, for ultracold Fermi gases of spin- F atoms, the generalization of Lee-Huang-Yang pseudo-potential that describes the two-particle collisions in the s-wave channel reads [77]:

$$U_1 = \sum_{J=0,2,\dots}^{2F-1} \frac{g_J}{2V} \sum_{M=-J}^J \sum_{\alpha\beta\gamma\delta} \langle FF\alpha\beta | JM \rangle \langle JM | FF\gamma\delta \rangle \times \sum_{p\mathbf{k}q\mathbf{r}} c_{p\alpha}^\dagger c_{k\beta}^\dagger c_{q\gamma} c_{r\delta} \delta_{p+\mathbf{k},q+\mathbf{r}}, \quad (4)$$

where $\langle \alpha\beta | FFmJ \rangle$ are Clebsch-Gordan coefficients. The couplings that parametrize the short-range interaction are $g_J = 8\pi a_s^J/m$, where a_s^J are the s-wave scattering lengths of the scattering channel with total spin J , m is the atom mass and V is the volume of the system. However, before the quench the AEAs in their ground state interact with an interaction for which all scattering lengths a_s^J are identical with very high accuracy, which results in the emergent SU(N) symmetry [1–3] mentioned above. Thus, the initial interaction reads:

$$U_0 = \frac{g_i}{2V} \sum_{p\mathbf{k}q\mathbf{r}} c_{p\alpha}^\dagger c_{k\beta}^\dagger c_{q\beta} c_{r\alpha} \delta_{p+\mathbf{k},q+\mathbf{r}}, \quad (5)$$

where the coupling $g_i = 8\pi a_s/m$, a_s being the scattering length. However, suddenly turning on U_1 which contains different values of g_J (i.e. $g_0 \neq g_2 \neq \dots$) breaks the SU(N) symmetry while respecting spin rotation symmetry. This means that in the two-particle scattering events, the total (hyperfine) spin of the colliding particles is still conserved but the spins of the colliding particles

can change. In the latter case, we speak of spin changing collisions (SCCs, see Fig. 1, right panel).

Unfortunately, for gases of AEAs the kind of interaction quench envisaged above that breaks the emergent $SU(N)$ symmetry cannot be realized using magnetic Feshbach resonances because the latter are not accessible in the ground state due to their closed-shell electronic structure. However, by means of the so-called optical Feshbach resonances (OFR) [4, 78–84] it is possible to (suddenly) enhance the values of the scattering lengths a_s^J . To this end, a laser is used to couple a pair of colliding atoms with an excited bound state, which induces a Feshbach resonance and modifies the scattering lengths a_s^J . This method for enhancing the interaction violates the emergent $SU(N)$ symmetry of the resulting interaction since the ground state is coupled to an excited state that possess a hyperfine structure. As a result, it should be possible to observe the dynamics of the initially $SU(N)$ -symmetric gas that is subject to an $SU(N)$ -symmetry breaking interaction quench. The price to pay for the use of OFR is the introduction of inelastic losses, which result from the real excitation to the excited bound state of a pair of AEAs. Inelastic losses will provide an additional mechanism for the suppression of pre-thermalization. However, in our theoretical study, we shall neglect their effect in order to understand the effects of elastic interactions alone, which is a good approximation provided the gas is not driven too close to the resonant regime of the OFR. The latter condition is also consistent with the perturbative approach that we use below, which requires that the interaction couplings g_J are not too large, and with the numerical observation that pre-thermalization is most observed in the weak to intermediate coupling regime [67, 74].

Following previous work [29–32, 39, 45, 46, 74, 75, 85, 86], we shall study the evolution of the instantaneous momentum distribution and the total energy in order to identify the pre-thermalized regime, i.e. we compute:

$$n_{p\sigma}(t) = \langle \Psi(t) | c_{p\sigma}^\dagger c_{p\sigma} | \Psi(t) \rangle, \quad (6)$$

$$E_{\text{tot}}(t) = \langle \Psi(t) | H(t) | \Psi(t) \rangle, \quad (7)$$

where $|\Psi(t)\rangle$ is the solution of the time-dependent Schrödinger equation for the Hamiltonian $H(t)$ (cf. Eq. 2). In the following section, we compute the short-time dynamics of $n_{p\sigma}(t)$ using perturbation theory to the lowest non-trivial orders in the initial and quench interactions. The second order results obtained below are valid for times that fulfill the condition [30, 31] $\epsilon_F t \lesssim (g_{\text{max}}^J k_F^3 / \epsilon_F)^{-3} \simeq (k_F a_{\text{max}}^J)^{-3}$, where g_{max}^J (a_{max}^J) is the largest coupling (scattering length) in the quenched interaction and ϵ_F (k_F) is the mean Fermi energy (momentum).

From the instantaneous momentum distribution, we obtain the total particle number of each spin-component,

$$N_\sigma(t) = \sum_p n_{p\sigma}(t), \quad (8)$$

as well the discontinuity of the momentum distribution at Fermi momentum:

$$Z_\sigma(t) = \lim_{\delta \rightarrow 0^+} [n_{p_{F\sigma} + \delta, \sigma}(t) - n_{p_{F\sigma} - \delta, \sigma}(t)]. \quad (9)$$

Below, when discussing pre-thermalization, we will focus on $Z_\sigma(t)$ rather than on the full momentum distribution.

For a sudden quench, the dynamics of total energy can be obtained by resorting to energy conservation. Consider the evolution of the total energy for times $t > 0$: The state of the system is described by $|\Psi(t)\rangle = e^{-i(H_0 + U_1)t} |\Psi(0)\rangle$. Hence,

$$E_{\text{tot}}(t > 0) = \langle \Psi(t) | H(t) | \Psi(t) \rangle \quad (10)$$

$$= \langle \Psi(0) | (H_0 + U_1) | \Psi(0) \rangle \quad (11)$$

$$= E_0 + \langle \Psi(0) | U_1 | \Psi(0) \rangle, \quad (12)$$

where $E_0 = \langle \Psi(0) | H_0 | \Psi(0) \rangle$. In other words, the total energy is a constant for $t > 0$, and for any time t , it exhibits rather simple evolution dynamics:

$$E_{\text{tot}}(t) = E_0 + \theta(t) \langle \Psi(0) | U_1 | \Psi(0) \rangle. \quad (13)$$

The above result implies that the total energy immediately reaches its final (thermal) value after the quench. For a Dirac-delta interaction (also called single-channel model), it is not possible to mathematically define the instantaneous kinetic energy. This is because the instantaneous momentum distribution $n_{k\sigma}(t)$ behaves as k^{-4} for $k \gg k_F$ [76], which renders the integral $E_{\text{kin}} = \sum_{k,\sigma} \epsilon_k n_{k\sigma}(t)$ divergent. Thus, we shall define the pre-thermalized regime as a state in which the total energy has reached its (final) thermal value whilst the momentum distribution has not. This means that the existence of a pre-thermalized regime can entirely be inferred from the existence, for certain time following the quench, of a quasi-stationary, non-thermal momentum distribution. In Fermi systems, this is manifested by a plateau in the evolution of the instantaneous discontinuity at the Fermi momentum, $Z_\sigma(t)$ (cf. Eq. 9).

III. INSTANTANEOUS MOMENTUM DISTRIBUTION

In this section, we describe how the time evolution of the instantaneous momentum distribution is obtained. Assuming that the interaction strength is weak, we shall compute the evolution of a given observable O in a perturbative series in the total interaction, $V(t) = e^{iKt} [U_0(t) + U_1(t)] e^{-iKt}$, where we used that the initial interaction $U_0(t) = U_0 e^{-\eta|t|}$ is adiabatically switched on

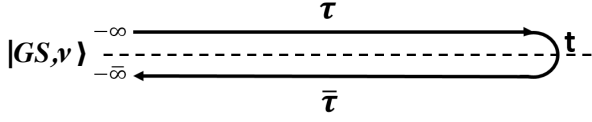


FIG. 2. Closed-time contour C . Times τ and $\bar{\tau}$ lie on the time ordered and anti-time ordered branches, respectively. τ is earlier than $\bar{\tau}$ in contour ordering. The turning point t is the time of at which observable in which we are interested is evaluated. $|GS, \nu\rangle$ is the initial state, which we take to be the ground state of non-interacting N -component Fermi gas characterized by a certain population ratio ν (see discussion below).

(off) at a rate $\eta \rightarrow 0^+$. Thus,

$$\begin{aligned} O(t) &= \frac{\langle GS, \nu | \mathcal{T} [e^{-i \int_C dt V(t)} O(t)] | GS, \nu \rangle}{\langle GS, \nu | \mathcal{T} [e^{-i \int_C dt V(t)}] | GS, \nu \rangle} \quad (14) \\ &= \langle O \rangle - i \int_C dt_1 \langle \mathcal{T} [V(t_1) O(t)] \rangle \\ &\quad + \frac{(-i)^2}{2!} \int_C dt_1 dt_2 \langle \mathcal{T} [V(t_1) V(t_2) O(t)] \rangle_c \\ &\quad + \dots \quad (15) \end{aligned}$$

where $\langle O \rangle = \langle GS, \nu | O | GS, \nu \rangle$. The times t_1, t_2, \dots all lie on the closed contour C shown in Fig. 2 and \mathcal{T} is the time-ordering symbol on C . The state $|GS, \nu\rangle$ denotes a non-interacting state, which is characterized by a particular ratio ν of the population of the different spin components (the definition of ν depends on the number of components, see below). Strictly speaking, the denominator of Eq. (14) equals unity, but it is needed when expanding in powers of $V(t)$ in order to cancel disconnected terms resulting from the application of Wick's theorem to the above expression.

Previous work [30–32, 39, 45, 46, 74, 75, 85, 86] has established that pre-thermalization is accessible through perturbation theory. In the problem of interest here, the perturbation series for the observable O can be organized as a double perturbative expansion in powers of U_0 and U_1 , i.e.

$$\begin{aligned} \langle O(t) \rangle &= O^{(0,0)} + O^{(0,1)}(t) + O^{(1,0)} \\ &\quad + O^{(1,1)} + O^{(0,2)}(t) + O^{(2,0)}(t) + \dots \quad (16) \end{aligned}$$

where $O^{(n,m)}(t)$ denotes the term that is n -th order in the initial interaction U_0 and m -th order in quenched interaction, U_1 . Next we set $O = c_{\mathbf{p}\sigma}^\dagger c_{\mathbf{p}\sigma}$, and thus,

$$\begin{aligned} n_{\mathbf{p}\sigma}(t) &= n_{\mathbf{p}\sigma}^{(0,0)}(t) + n_{\mathbf{p}\sigma}^{(1,0)}(t) + n_{\mathbf{p}\sigma}^{(0,1)}(t) \\ &\quad + n_{\mathbf{p}\sigma}^{(1,1)}(t) + n_{\mathbf{p}\sigma}^{(2,0)}(t) + n_{\mathbf{p}\sigma}^{(0,2)}(t) + \dots \quad (17) \end{aligned}$$

where $n_{\mathbf{p}\sigma}^{(0,0)}(t) = n_{\mathbf{p}\sigma}^0$. In the closed time contour C , we can express the other $n_{\mathbf{p}\sigma}^{(n,m)}(t)$ in terms of the self-energy and propagator matrices which, to second order

in the total interaction, read:

$$\begin{aligned} n_{\mathbf{p}\sigma}^{(1,0)}(t) &= \int_C dt_1 \mathcal{G}_{\mathbf{p}\sigma}(t, t_1) \Sigma_{\mathbf{p}\sigma}^{(0,1)}(t_1) \mathcal{G}_{\mathbf{p}\sigma}(t_1, t), \\ n_{\mathbf{p}\sigma}^{(0,2)}(t) &= \int_C dt_1 \mathcal{G}_{\mathbf{p}\sigma}(t, t_1) \Sigma_{\mathbf{p}\sigma}^{(0,1)}(t_1) \mathcal{G}_{\mathbf{p}\sigma}(t_1, t), \\ n_{\mathbf{p}\sigma}^{(2,0)}(t) &= \int_C dt_1 dt_2 \mathcal{G}_{\mathbf{p}\sigma}(t, t_2) \Sigma_{\mathbf{p}\sigma}^{(2,0)}(t_2, t_1) \mathcal{G}_{\mathbf{p}\sigma}(t_1, t), \\ n_{\mathbf{p}\sigma}^{(1,1)}(t) &= \int_C dt_1 dt_2 \mathcal{G}_{\mathbf{p}\sigma}(t, t_2) \Sigma_{\mathbf{p}\sigma}^{(1,1)}(t_2, t_1) \mathcal{G}_{\mathbf{p}\sigma}(t_1, t). \quad (18) \end{aligned}$$

The propagator $\mathcal{G}_{\mathbf{p}\sigma}(a, b)$ is defined in Eq. (A2), and $\Sigma_{\mathbf{p}\sigma}^{(1)}(t_1)$, $\Sigma_{\mathbf{p}\sigma}^{(2)}(t_2, t_1)$ can be computed using Feynman diagrams (see Appendix A).

For the calculation of equal-time expectation values, we choose the time argument of the observable (t) to lie slightly before the turning point of the contour C , which is on the time ordered (τ) branch. In this case, the fermion propagators must be obtained from Eq. (A1), which yields:

$$\mathcal{G}_{\mathbf{p}\sigma}(t, b) = e^{-i\epsilon_p(t-b)} \begin{pmatrix} 1 - n_{\mathbf{p}\sigma}^0 & -n_{\mathbf{p}\sigma}^0 \\ 0 & 0 \end{pmatrix}, \quad (19)$$

where the non-vanishing entries correspond to either b lying before or after t on the contour C . Similarly,

$$\mathcal{G}_{\mathbf{p}\sigma}(a, t) = e^{-i\epsilon_p(a-t)} \begin{pmatrix} -n_{\mathbf{p}\sigma}^0 & 0 \\ 1 - n_{\mathbf{p}\sigma}^0 & 0 \end{pmatrix}. \quad (20)$$

and the two non-zero entries correspond to a lying before or after t on the contour C . Combining Eq. (17), the propagators, Eq. (19) and Eq. (20) and the second order corrections to the self-energy, Eqs. (A17) to (A20), we arrive at:

$$\begin{aligned} n_{\mathbf{p}\sigma}^{(2)}(t) &= -\frac{2}{V^2} \sum_{\alpha\beta\gamma} \sum_{\mathbf{p}\mathbf{k}\mathbf{q}\mathbf{r}} Q_{\mathbf{p}\mathbf{k}\mathbf{q}\mathbf{r}}^{\sigma\alpha\beta\gamma} \int_{-\infty}^t dt_1 \int_{-\infty}^t dt_2 e^{iE_{\mathbf{p}\mathbf{k}\mathbf{q}\mathbf{r}}(t_1-t_2)} \\ &\quad \times \left[g_f^{(2)}(\sigma, \alpha; \beta, \gamma) \theta(t_1) \theta(t_2) + g_i^2 \delta_{\sigma,\beta} \delta_{\alpha,\gamma} e^{-\eta(|t_1|+|t_2|)} \right. \\ &\quad \left. + 2g_i g_f^{(1)}(\sigma, \alpha; \sigma, \alpha) \delta_{\sigma,\beta} \delta_{\alpha,\gamma} \theta(t_1) e^{-\eta|t_2|} \right], \\ &= -\frac{2}{V^2} \sum_{\mathbf{k}\mathbf{q}\mathbf{r}} \sum_{\alpha\beta\gamma} Q_{\mathbf{p}\mathbf{k}\mathbf{q}\mathbf{r}}^{\sigma\alpha\beta\gamma} \left\{ \frac{g_i^2 \delta_{\sigma,\beta} \delta_{\alpha,\gamma}}{E_{\mathbf{p}\mathbf{k}\mathbf{q}\mathbf{r}}^2} + \left[g_J^{(2)}(\sigma, \alpha; \beta, \gamma) \right. \right. \\ &\quad \left. \left. + g_i g_J^{(1)}(\sigma, \alpha; \sigma, \alpha) \delta_{\sigma,\beta} \delta_{\alpha,\gamma} \right] F(E_{\mathbf{p}\mathbf{k}\mathbf{q}\mathbf{r}}, t) \right\}, \quad (21) \end{aligned}$$

where we have defined $E_{\mathbf{p}\mathbf{k}\mathbf{q}\mathbf{r}} = \epsilon_p + \epsilon_k - \epsilon_q - \epsilon_r$ and introduced $F(E, t)$ to denote the result of the integration over t_1 and t_2 :

$$F(E, t) = \frac{4 \sin^2(Et/2)}{E^2}. \quad (22)$$

In Eq. (21) $Q_{pkqr}^{\sigma\alpha\beta\gamma}$ corresponds to the following expression:

$$Q_{pkqr}^{\sigma\alpha\beta\gamma} = \delta_{p+k,q+r} \left[n_{p\sigma}^0 n_{k\alpha}^0 (1 - n_{q\beta}^0) (1 - n_{r\gamma}^0) - (1 - n_{p\sigma}^0) (1 - n_{k\alpha}^0) n_{q\beta}^0 n_{r\gamma}^0 \right]. \quad (23)$$

IV. TWO-COMPONENT FERMI GAS

As a warm up, in this section we consider the two component gas in order to show that breaking the $SU(N=2)$ symmetry of the initial state by introducing an initial population imbalance does not suppress pre-thermalization.

Let us first recall that for a contact interaction in a two-component system, the pseudo-potential in Eq. (4) is parametrized by a *single* coupling constant only, which is determined by the s-wave scattering length for atoms colliding with total $J=0$, a_s . Therefore, it is not possible to break the $SU(N=2)$ symmetry of the interaction. Indeed, as shown in Fig. 3, the only scattering process in a two-component gas is of the type $(\uparrow + \downarrow) \rightarrow (\uparrow + \downarrow)$. This kind of scattering process preserves the populations of each spin component. Thus, even if the initial state contains an population imbalance (i.e. for $\nu = N_\uparrow/N_\downarrow \neq 1$), the time evolution following the quench cannot alter the ratio ν . This conservation law alone protects the existence of the pre-thermalized regime.

In order to show that pre-thermalization is preserved, we have evaluated explicitly the time evolution of the discontinuity of the instantaneous momentum distribution at Fermi momenta, i.e. $Z_\sigma(t)$, see Fig. 4. Notice that, after a short transient, $Z_\sigma(t)$ displays a plateau for both spin components. This is a behavior characteristic of the pre-thermalized regime indicating that the momentum distribution is non-thermal, similarly to what was found in previous studies using different models and spin-unpolarized initial states [29, 30, 32, 74]. The initial population imbalance is reflected in the pre-thermal

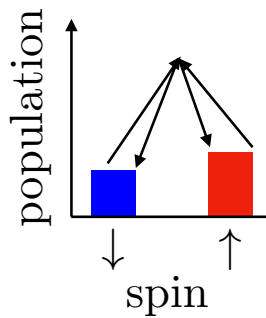


FIG. 3. Schematic representation of the only scattering process allowed in a two-component gas with Dirac-delta interactions. Notice that $(\uparrow + \downarrow) \rightarrow (\uparrow + \downarrow)$, thus preserving the spin-populations for each spin component.

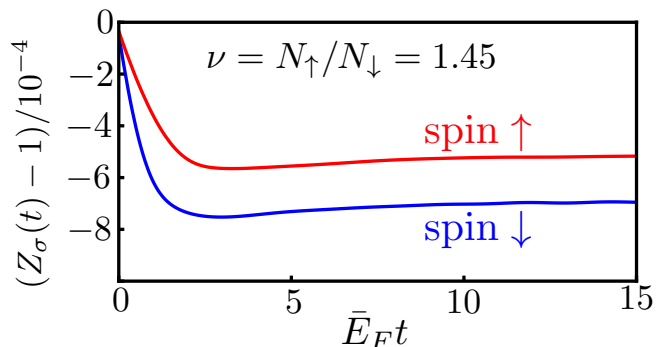


FIG. 4. (color online) Dynamics of discontinuity of the momentum distribution at Fermi momentum $Z_\sigma(t)$ after a sudden interaction quench in a two-component Fermi gas. After a short transient, a plateau is observed indicating the existence of a pre-thermalized regime. Time is measured in units of the inverse of mean Fermi energy, $\bar{E}_F = (\epsilon_F^\uparrow + \epsilon_F^\downarrow)/2 = \bar{k}_F^2/2m$. The interaction strength is $\bar{k}_F a_s^0 = 0.0158$ for the quenched interaction and we take $\bar{k}_F a_s = 0.0097$ for the initial interaction.

value of $Z_\uparrow(t)$ being different from that of $Z_\downarrow(t)$. Indeed, we have checked that this result also applies to $N > 2$ -component Fermi gas. Thus, we conclude that, if the post-quench Hamiltonian retains the $SU(N)$ symmetry, the system shows pre-thermalization independently of the existence of population imbalance in the initial state (see discussion in the following section).

Next we consider the effects of the initial interaction. Although the latter is $SU(N=2)$ symmetric and therefore will not suppress pre-thermalization, for the sake of experimental interest, it is worth analyzing its quantitative effect on the dynamics of the instantaneous momentum distribution. As a function of the ratio a_s/a_s^0 Fig. 5 shows the ratio of the pre-thermalized value of $Z_\uparrow(t)$ to its value in the ground state of $H_0 + U_1 = K + U_0 + U_1$ (see Appendix A for the details of the calculation). Recall that the (initial) interaction strength is $g_i = 8\pi a_s/m$ and a_s^0 is the scattering length characterizing the quench interaction strength $g_0 = 8\pi a_s^0/m$. Thus, the final interaction is proportional to $8\pi(a_s + a_s^0)/m$. The inset shows the full time dependence for a few values of the ratio a_s/a_s^0 . The results shown in Fig. 5 can be summarized by the following relation:

$$\frac{1 - Z_\sigma^{\text{st}}}{1 - Z_\sigma^{\text{eq}}} = C\left(\frac{a_s}{a_s^0}\right), \quad (24)$$

where the crossover function $C(x)$ takes the following limiting forms: $C(x \gg 1) = 1$ and $C(x \ll 1) = 2$, while interpolating in between for intermediate values of $x = a_s/a_s^0$. The $x \rightarrow 0$ limit, which corresponds to the non-interacting initial state, has been obtained in previous work [30–32].

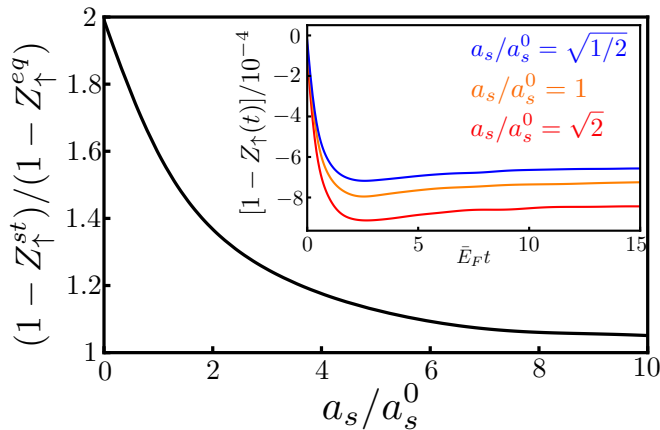


FIG. 5. Ratio of the stationary and equilibrium values of the discontinuity at the Fermi momentum of the momentum distribution, Z_{σ} , for the spin $\sigma = \uparrow$ in a two-component Fermi gas following a sudden interaction quench where a_s^0 is the scattering length of the quenched interaction, and a_s^0 is the scattering length of the initial interaction. The post-quench total scattering length is $a_s + a_s^0$. As discussed in the main text, the ratio $(1 - Z_{\uparrow}^{st}) / (1 - Z_{\uparrow}^{eq})$ ranges between 1 and 2 and depends on the ratio of the initial to the final interaction strengths. The inset shows the evolution of discontinuity at Fermi momentum for different values of the ratio a_s / a_s^0 . The interaction strength for the quenched interaction is $\bar{k}_F a_s^0 = 0.0158$. Time is measured in units of the inverse of the mean Fermi energy $\bar{E}_F = (\epsilon_{\uparrow}^{\uparrow} + \epsilon_{\uparrow}^{\downarrow}) / 2 = \bar{k}_F^2 / 2m$.

V. SUPPRESSION OF PRE-THERMALIZATION

The dynamics of the two-component gas described above illustrates that introducing a population imbalance in the initial state is not a sufficient condition to suppress pre-thermalization. In this section, we show that the situation changes dramatically when, besides the initial population imbalance, we allow for spin-changing collisions (SCCs) that result from the breaking of the $SU(N)$ symmetry of the quenched interaction. For a contact interaction that conserves the total angular momentum, the minimum value of N allowing for SCCs is $N = 4$. Fig. 1 schematically shows the two possible types of scattering processes. They are classified into two types: those preserving the relative spin populations (left panel) and the SCCs (right panel).

Next, we consider a sudden interaction quench in an initially interacting (with scattering length a_s) four-component Fermi gas. We assume the initial state contains an imbalance in the population of the different spin components as shown in Fig. 1. This population imbalance can be parametrized by the ratio $\nu = N_{\pm 1/2} / N_{\pm 3/2}$, which also determines the non-interacting state $|GS, \nu\rangle$ used in the perturbative treatment outlined in Sec. A. On the left panel of Fig. 6 we have plotted the time evolution of $Z_{\sigma}(t)$ for $\nu = 1.45$. In this case, unlike the plateau observed for the *imbalanced* two-component gas, we find a slow decay of $Z_{\sigma}(t)$ as a function of time, which is indica-

tive of the absence of pre-thermalization. In order to shed further light into the behavior of the system, it is useful to consider the dynamics of the ratio $\delta N_{\pm 3/2}(t) / N_{\text{tot}}$, where $\delta N_{\sigma}(t)$ measures the deviation from its initial value of the population for spin component σ . This ratio is shown in Fig. 6, which illustrates how the SCCs alter the relative populations by decreasing the population of the majority components with $\sigma = \pm 1/2$ and increasing that of the minority component (note that $\delta N_{\pm 1/2}(t) = -\delta N_{\pm 3/2}(t)$ because the total number is conserved). This change in relative population is the driving force behind the change of the kinetic energy for the components with $\sigma = \pm 3/2$ and $\sigma = \pm 1/2$.

Analytically (see Appendix B), it can be shown that, after a short transient, the rate of population change is given by Fermi's Golden rule. This result can be obtained by formally taking the limit $t \rightarrow +\infty$ of the second order expressions for $\delta N_{\sigma}(t)$, i.e.

$$\begin{aligned} \lim_{t \rightarrow \infty} \frac{\delta N_{\sigma}(t)}{t} &\propto \frac{1}{V^2} \sum_{\mathbf{p}\mathbf{k}\mathbf{q}\mathbf{r}} \sum_{\alpha\beta\gamma} g_f^{(2)}(\sigma, \alpha; \beta, \gamma) [n_{\mathbf{p}\sigma}^0 n_{\mathbf{k}\alpha}^0 \\ &\times (1 - n_{\mathbf{q}\beta}^0)(1 - n_{\mathbf{r}\gamma}^0) - (1 - n_{\mathbf{p}\sigma}^0)(1 - n_{\mathbf{k}\alpha}^0)n_{\mathbf{q}\beta}^0 n_{\mathbf{r}\gamma}^0] \\ &\times \delta(\epsilon_{\mathbf{p}} + \epsilon_{\mathbf{k}} - \epsilon_{\mathbf{q}} - \epsilon_{\mathbf{r}}) \delta_{\mathbf{p}+\mathbf{k}, \mathbf{q}+\mathbf{r}}, \end{aligned} \quad (25)$$

where $g_f^{(2)}(\sigma, \alpha; \beta, \gamma)$ is the (square of the) matrix element for SCCs.

Note that the rate of population change is independent of the initial $SU(N)$ -symmetric interaction. The slope is proportional to the phase space volume available for SCCs multiplied by the matrix element mediating the transitions. Thus, this rate can be used as a measure of how severe the suppression of pre-thermalization is. As shown in Fig. 6, the rate of change of $\delta N_{\sigma}(t)$ (that is, its slope in Fig. 6) becomes larger as the initial population imbalance increases, as expected from the corresponding enhancement in the available phase space. Since the SCCs induce inelastic scattering processes, they provide a decoherence mechanism in the short time dynamics after the quench. Thus, for an initial state with $\nu \neq 1$ in the presence of SCCs, neither the relative population nor the momentum distribution for each spin component become stationary after a short-time transient, indicating that the intermediate time behavior cannot be described as pre-thermal. Conversely, the pre-thermalized regime is robust when inelastic scattering processes are (Pauli-)blocked at short time, which is the case of an initial state with no spin imbalance (i.e. $\nu = 1$), or when the SCCs are absent because the quenched interaction is $SU(N)$ symmetric.

VI. CONTROL OF PRE-THERMALIZATION

We have seen in the previous sections that pre-thermalization can take place provided the symmetries of the post-quench Hamiltonian or the initial state are properly broken. Here we demonstrate the possibility of

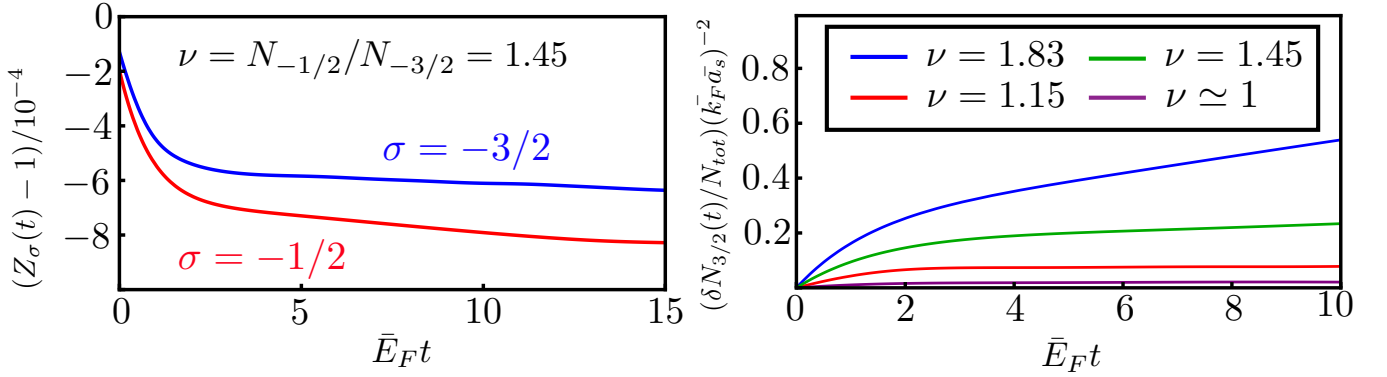


FIG. 6. (color online) **Left panel:** Dynamics of the discontinuity at Fermi momentum of the momentum distribution for a $N = 4$ Fermi gas following a sudden quench of the interaction that breaks the $SU(4)$ symmetry. The population ratio in the initial state $\nu = N_{\pm 1/2}/N_{\pm 3/2} = 1.45$. **Right panel:** Evolution of the population ratio $\delta N_{\sigma}/N_{tot}(\bar{k}_F \bar{a}_s)^{-2}$ for $\sigma = 3/2$, and different initial conditions with symmetry ($N_{1/2} = N_{-1/2}$, $N_{3/2} = N_{-3/2}$). Time is measured in units of the inverse of the mean Fermi energy $\bar{E}_F = (\epsilon_F^{3/2} + \epsilon_F^{1/2})/2 = \bar{k}_F^2/2m$. The interaction strength determined by the parameters $\bar{k}_F a_s^0 = 0.0158$ and $\bar{k}_F a_s^2 = 0.0032$, for the quenched interaction, and $\bar{k}_F a_s = 0.0097$ for the initial interaction, respectively.

controlling the existence of pre-thermalization by carefully choosing the initial state.

As mentioned above, Eq. (25) shows that the rate of change of the relative populations vanishes when the population of the different spin species is the same and the initial state becomes $SU(N = 4)$ symmetric. However, this is not the only type of initial condition for which the rate of change of relative populations vanishes. Indeed, it is possible to find other types of initial states for which the rate of change of the relative population, Eq. (25) vanishes. To see this, let us define $E_{p\alpha} = \epsilon_p - \epsilon_F^\alpha$, where ϵ_F^α is the Fermi energy for the component α . Thus, the Dirac delta function, ensuring energy conservation in Eq. (25) becomes:

$$\delta(\epsilon_p + \epsilon_k - \epsilon_q - \epsilon_r) = \delta(E_{p\sigma} + E_{k\alpha} - E_{q\beta} - E_{r\gamma} + \Delta_F) \quad (26)$$

where $\Delta_F = \epsilon_F^\sigma + \epsilon_F^\alpha - \epsilon_F^\beta - \epsilon_F^\gamma$. In addition, we notice that $\delta N(t)$ receives contributions only from the SCCs, which for $N = 4$ means that $\sigma = -\alpha = \frac{3}{2}$ and $\beta = -\gamma = \frac{1}{2}$. Thus,

$$\Delta_F = \epsilon_F^{+3/2} + \epsilon_F^{-3/2} - \epsilon_F^{+1/2} - \epsilon_F^{-1/2}. \quad (27)$$

Next we shall argue that initial states satisfying $\Delta_F = 0$, will exhibit pre-thermal behavior (when initial interactions are present, the initial state must be adiabatically connected to a non-interacting state that satisfies the condition $\Delta_F = 0$ since the initial $SU(N)$ -symmetric interaction does not induce SCCs). In order to establish this result, we first notice that the expression in Eq. (25) contains two terms. In the first one, the occupation factors $n_{p\sigma}^0 n_{k\alpha}^0 (1 - n_{q\beta}^0)(1 - n_{r\gamma}^0)$ require, at $T = 0$, that is, for a pure state, that $E_{p\sigma}, E_{k\alpha} \geq 0$ and $E_{q\beta}, E_{r\gamma} \leq 0$. At the same time, the energy conservation for $\Delta_F = 0$ requires that $E_{p\sigma} + E_{k\alpha} = E_{q\beta} + E_{r\gamma}$, which can only be satisfied if $E_{p\sigma} = E_{k\alpha} = E_{q\beta} = E_{r\gamma} = 0$. The manifold of points satisfying the previous condition in

the nine-dimensional space span by the vectors $\mathbf{p}, \mathbf{k}, \mathbf{q}$ ($\mathbf{r} = \mathbf{p} + \mathbf{k} - \mathbf{q}$ is fixed by momentum conservation) is a set of zero measure and does not contribute to the integrals over momentum in Eq. (25). An entirely identical conclusion is reached for the second term in Eq. (25). Physically, the condition that $\Delta_F = 0$ amounts to having zero phase space for the SCCs to occur, even if this is not obvious from the fact that the initial state contains a population imbalance. This argument can be easily generalized to the case where $N > 4$.

In order to explicitly show how pre-thermal behavior emerges when $\Delta_F = 0$, we have computed the evolution of $Z_\sigma(t)$ and $\delta N_{\sigma(t)}$ by numerically evaluating the corresponding expressions for an initial state satisfying the condition that $\Delta_F = 0$. The results are shown in Fig. 7. It is worth comparing the results on the right panel of Fig. 7, with those shown in Fig. 7 (left panel). It can be seen that, after a short transient, for the initial state satisfying the condition $\Delta_F = 0$, the curves for $\delta N_{\sigma(t)}$ flatten out. Concurrently, $Z_\sigma(t)$ also reaches the characteristic pre-thermal plateau. However, it is worth noticing that unlike the case of initial states with $SU(N)$ symmetry which trivially satisfy $\Delta_F = 0$, there is a change in population during the short-time transient because there are SCCs that do not satisfy energy conservation. The energy conservation is only enforced for t sufficiently large. When this happens, the system enters the pre-thermalized regime. As a caveat, it is important to notice that if change of population happens during the short-time transient, then condition $\Delta_F = 0$ will not ensure that the system reaches the pre-thermalized regime. Thus, we must require that $\delta N_{\sigma(t)}/N_{\sigma} \ll 1$, which is the case in the regime where quenched interaction can be treated perturbatively.

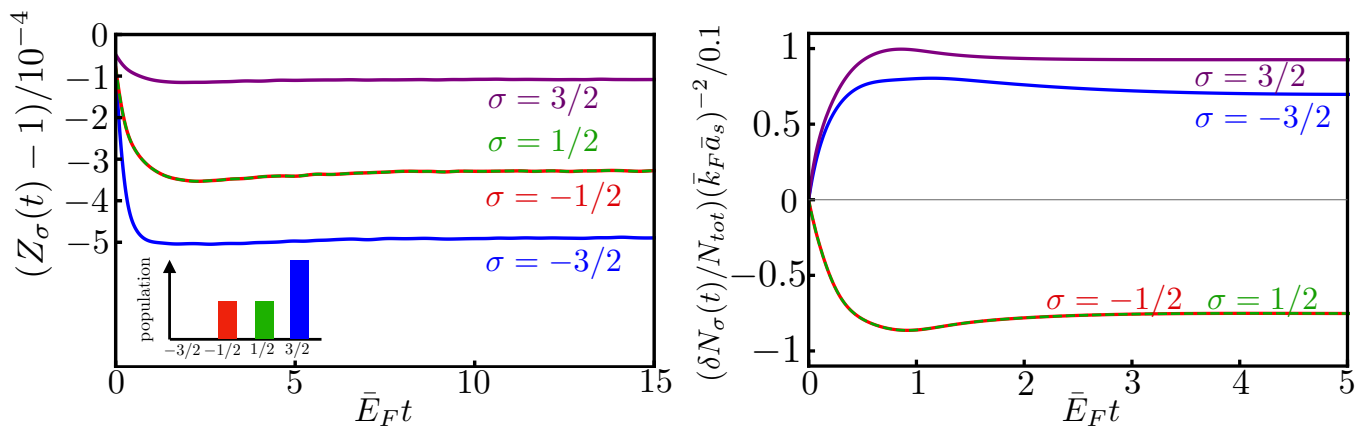


FIG. 7. (color online) **Left panel:** Discontinuity at the Fermi momentum starting from an imbalanced initial state. The plateau indicates the emergence of pre-thermalization in the presence of SCCs. The insertion shows the initial condition schematically where the imbalanced initial state is $\epsilon_F^{-3/2} = 0$ and $2\epsilon_F^{\pm 1/2} = \epsilon_F^{3/2}$. **Right panel:** Time-evolution of the relative population. After an initial exchange of particles, the spin populations reach stationary values. Time is measured in units of the inverse of the mean Fermi energy $\bar{E}_F = \frac{1}{4} \sum_{\sigma} \epsilon_F^{\sigma} = \bar{k}_F^2/2m$. The interaction strengths satisfy $\bar{k}_F a_s^0 = 0.0158$ and $\bar{k}_F a_s^2 = 0.0032$ (for the quenched interaction) and $\bar{k}_F a_s = 0.0097$ (for the initial interaction).

VII. CONCLUSIONS

In conclusion, we have studied the pre-thermalization dynamics of an isolated multi-component Fermi gas of ultracold atoms following a sudden interaction quench. This type of nonequilibrium dynamics can be experimentally studied using alkaline earth atoms, whose interaction can be tuned using optical Feshbach resonances [4, 78–81], e.g. in ^{173}Yb for $N \leq 6$ and ^{87}Sr for $N \leq 10$.

We have shown that the short-time dynamics of this system is affected by both the presence of a population imbalance in the initial state and the breaking of the emergent $\text{SU}(N)$ symmetry of the contact interactions by allowing spin-changing collisions. Both elements are necessary for the suppression of pre-thermalization, as illustrated by the behavior of two-component Fermi gas with initial spin imbalance, which displays a robust pre-thermalized regime at short to intermediate times. On the other hand, for a generic $\text{SU}(N \geq 4)$ symmetry-breaking (i.e. imbalanced) initial state we do not observe a pre-thermal regime after a quenching an $\text{SU}(N)$ -symmetry-breaking interacting. This is because, generically, the population imbalance in the initial state provides phase space for inelastic spin-changing collisions and introduces a decoherence mechanism and suppress pre-thermalization.

Nevertheless, we have shown that there is a class of imbalanced initial states which allows for the emergence of pre-thermal behavior. This opens the possibility of using multi-component gases to study the suppression and control of this nonequilibrium state. In addition, the findings reported in this work should allow for the possibility to experimentally observe the effect of SCCs by studying the dynamics of the quantum gas following

an interaction quench.

ACKNOWLEDGMENTS

MAC and CHH have been supported by the Ministry of Science and Technology (Taiwan) under contract numbers NSC 102- 2112-M-007-024-MY5 and 107-2112-M-007-021-MY5. MAC also acknowledges the support of the National Center for Theoretical Sciences (NCTS) of Taiwan. YT and YT acknowledge the supports by the Grant-in-Aid for Scientific Research of the Ministry of Education, Culture Sports, Science, and Technology / Japan Society for the Promotion of Science (MEXT/JSPS KAKENHI) Nos. 25220711 and 17H06138, 18H05405, and 18H05228; the Impulsing Paradigm Change through Disruptive Technologies (ImPACT) program; Japan Science and Technology Agency CREST (No. JPMJCR1673), and MEXT Quantum Leap Flagship Program (MEXT Q-LEAP)(JPMXS0118069021).

Appendix A: Technical details of the calculations

The fully connected contributions (denoted by $\langle \dots \rangle_c$ in Eq. 15) resulting from the application of Wick's theorem can be represented in terms of Feynman graphs (cf Fig. 8). Notice that there are four possible choices for the time arguments for the fermion propagator:

$$iG_0(t_1, t_2; p\sigma) = \langle \mathcal{T} [c_{p\sigma}(t_1) c_{p\sigma}^\dagger(t_2)] \rangle, \quad (\text{A1})$$

where t_1 and t_2 can be either in the τ or $\bar{\tau}$ branches of C . The free fermion propagator can be written in matrix

form as follows:

$$\mathcal{G}_{p\sigma}(a, b) = \begin{pmatrix} iG_{p\sigma}^T(a, b) & iG_{p\sigma}^<(a, \bar{b}) \\ iG_{p\sigma}^>(\bar{a}, b) & iG_{p\sigma}^T(\bar{a}, \bar{b}) \end{pmatrix}. \quad (\text{A2})$$

Using $c_{p\sigma}(t) = c_{p\sigma}e^{-i\epsilon_p t}$, the entries of above matrix can be evaluated to yield:

$$iG_{p\sigma}^<(t_1, \bar{t}_2) = -n_{p\sigma}^0 e^{i\epsilon_p(t_2-t_1)}, \quad (\text{A3})$$

$$iG_{p\sigma}^>(\bar{t}_1, t_2) = (1 - n_{p\sigma}^0) e^{i\epsilon_p(t_2-t_1)}, \quad (\text{A4})$$

$$iG_{p\sigma}^T(t_1, t_2) = \theta(t_1 - t_2) iG_{p\sigma}^>(\bar{t}_1, t_2) + \theta(t_2 - t_1) iG_{p\sigma}^<(t_1, \bar{t}_2); \quad (\text{A5})$$

$$iG_{p\sigma}^{\bar{T}}(\bar{t}_1, \bar{t}_2) = \theta(t_2 - t_1) iG_{p\sigma}^>(\bar{t}_1, t_2) + \theta(t_1 - t_2) iG_{p\sigma}^<(t_1, \bar{t}_2). \quad (\text{A6})$$

For the calculation of equal-time expectation values, we choose the time argument of the operator (t) to lie slightly before the turning point of the contour C , which is on the time ordered (τ) branch. In this case, the fermion propagators must be obtained from Eq. (A1), which yields:

$$\mathcal{G}_{p\sigma}(t, b) = e^{-i\epsilon_p(t-b)} \begin{pmatrix} 1 - n_{p\sigma}^0 & -n_{p\sigma}^0 \\ 0 & 0 \end{pmatrix}, \quad (\text{A7})$$

where the non-vanishing entries correspond to either b lying before or after t on the contour C . Similarly,

$$\mathcal{G}_{p\sigma}(a, t) = e^{-i\epsilon_p(a-t)} \begin{pmatrix} -n_{p\sigma}^0 & 0 \\ 1 - n_{p\sigma}^0 & 0 \end{pmatrix}. \quad (\text{A8})$$

and the two non-zero entries correspond to a lying before or after t on the contour C .

The self-energy can be calculated from the diagrams shown in Fig. 8 and the propagators, Eqs. (A3) to (A6). Thus, to first order in $V(t)$, we obtain:

$$\Sigma_{\sigma}^{(0,1)}(t_1) = \frac{\theta(t_1)}{V} \sum_{\alpha} g_f^{(1)}(\sigma, \alpha; \sigma, \alpha) \sum_{\mathbf{k}} n_{\mathbf{k}\alpha}^0, \quad (\text{A9})$$

$$\Sigma_{\sigma}^{(1,0)}(t_1) = \frac{g_i}{V} \sum_{\alpha \neq \sigma} \sum_{\mathbf{k}} n_{\mathbf{k}\alpha}^0 e^{-\eta|t_1|}, \quad (\text{A10})$$

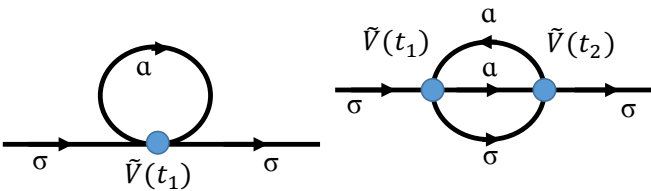


FIG. 8. First and second order diagram for momentum distribution. $V(t) = U_0(t) + U_1(t)$ is the sum of the total (initial plus quenched) interaction.

where we have introduced:

$$g_f^{(1)}(\sigma, \alpha; \sigma, \alpha) = \sum_{J=0,2,\dots} \sum_M g_J \langle JM | FF\sigma\alpha \rangle \langle FF\sigma\alpha | JM \rangle. \quad (\text{A11})$$

Combining the expression in matrix form, Eq. (17), the propagators, Eq. (A7) and Eq. (A8), and the self-energy for the first order correction, Eqs. (A9) and (A10), we obtain that first order correction to the instantaneous momentum distribution vanishes, i.e. $n_{p\sigma}^{(1)} = 0$.

At second order in the quenched interaction, we need to use the following self-energy matrix, which contains four different combinations of the time arguments (t_1, t_2) on the two branches of the closed contour:

$$\Sigma_{p\sigma}^{(2,0)}(b, a) = -\frac{2g_i^2}{V^2} e^{-\eta(|b|+|a|)} \sum_{\mathbf{k}\mathbf{q}\mathbf{r}} \delta_{\mathbf{p}+\mathbf{k}, \mathbf{q}+\mathbf{r}} \times \sum_{\alpha\beta\gamma} \bar{\Sigma}^{(2)}(b, a) \delta_{\sigma, \beta} \delta_{\alpha\gamma}, \quad (\text{A12})$$

$$\Sigma_{p\sigma}^{(1,1)}(b, a) = -\frac{4}{V^2} \theta(a) e^{-\eta|b|} \sum_{\mathbf{k}\mathbf{q}\mathbf{r}} \delta_{\mathbf{p}+\mathbf{k}, \mathbf{q}+\mathbf{r}} \times \sum_{\alpha\beta\gamma} g_i g_f^{(1)}(\sigma, \alpha; \sigma, \alpha) \bar{\Sigma}^{(2)}(b, a) \delta_{\sigma, \beta} \delta_{\alpha\gamma}, \quad (\text{A13})$$

$$\Sigma_{p\sigma}^{(0,2)}(b, a) = -\frac{2}{V^2} \theta(b) \theta(a) \sum_{\mathbf{k}\mathbf{q}\mathbf{r}} \delta_{\mathbf{p}+\mathbf{k}, \mathbf{q}+\mathbf{r}} \times \sum_{\alpha\beta\gamma} g_f^{(2)}(\sigma, \alpha; \beta, \gamma) \bar{\Sigma}^{(2)}(b, a), \quad (\text{A14})$$

where $\bar{\Sigma}^{(2)}(b, a)$ is the following matrix:

$$\bar{\Sigma}(b, a) = \begin{pmatrix} \bar{\Sigma}^{(2,T)}(b, a) & \bar{\Sigma}^{(2,>)}(\bar{b}, a) \\ \bar{\Sigma}^{(2,<)}(b, \bar{a}) & \bar{\Sigma}^{(2,\bar{T})}(\bar{b}, \bar{a}) \end{pmatrix} \quad (\text{A15})$$

where, for the sake of brevity, we have suppressed the explicit dependence of $\Sigma^{(2)}(b, a) = \Sigma_{\mathbf{k}\mathbf{q}\mathbf{r}, \alpha\beta\gamma}^{(2)}(b, a)$ on the momentum and spin indices. Furthermore, we have introduced the following notation:

$$g_f^{(2)}(\sigma, \alpha; \beta, \gamma) = \sum_{J_1, J_2=0,2,\dots} \sum_{M_1 M_2} g_{J_1} g_{J_2} \langle J_1 M_1 | FF\sigma\alpha \rangle \times \langle FF\beta\gamma | J_1 M_1 \rangle \langle J_2 M_2 | FF\sigma\alpha \rangle \langle FF\beta\gamma | J_2 M_2 \rangle, \quad (\text{A16})$$

which contains the information of coupling strength and Clebsch-Gordon coefficients. Using the diagram in Fig. 8 and free propagators in Eqs. (A11) to (A6), we can write down the following expression for the elements in the

matrix:

$$\begin{aligned}\bar{\Sigma}^{(2,<)}(t_2, \bar{t}_1) &= i^3 G_{k\alpha}^<(t_2, \bar{t}_1) G_{q\beta}^>(\bar{t}_1, t_2) G_{r\gamma}^>(\bar{t}_1, t_2), \\ &= (1 - n_{q\beta}^0)(1 - n_{r\gamma}^0) n_{k\alpha}^0 e^{i(t_1 - t_2)(\epsilon_q + \epsilon_r - \epsilon_k)},\end{aligned}\quad (\text{A17})$$

$$\begin{aligned}\bar{\Sigma}^{(2,>)}(\bar{t}_2, t_1) &= i^3 G_{k\alpha}^>(\bar{t}_2, t_1) G_{q\beta}^<(t_1, \bar{t}_2) G_{r\gamma}^<(t_1, \bar{t}_2), \\ &= n_{q\beta}^0 n_{r\gamma}^0 (1 - n_{k\alpha}^0) e^{i(t_1 - t_2)(\epsilon_q + \epsilon_r - \epsilon_k)},\end{aligned}\quad (\text{A18})$$

$$\begin{aligned}\bar{\Sigma}^{(2,T)}(t_2, t_1) &= i^3 G_{k\alpha}^T(t_2, t_1) G_{q\beta}^T(t_1, t_2) G_{r\gamma}^T(t_1, t_2), \\ &= \theta(t_2 - t_1) \Sigma^{(2,>)}(t_2, \bar{t}_1) + \theta(t_1 - t_2) \Sigma^{(2,>)}(\bar{t}_2, t_1),\end{aligned}\quad (\text{A19})$$

$$\begin{aligned}\bar{\Sigma}^{(2,\bar{T})}(\bar{t}_2, \bar{t}_1) &= i^3 G_{k\alpha}^{\bar{T}}(\bar{t}_2, \bar{t}_1) G_{q\beta}^{\bar{T}}(\bar{t}_1, \bar{t}_2) G_{r\gamma}^{\bar{T}}(\bar{t}_1, \bar{t}_2), \\ &= \theta(t_1 - t_2) \Sigma^{(2,>)}(t_2, \bar{t}_1) + \theta(t_2 - t_1) \Sigma^{(2,>)}(\bar{t}_2, t_1).\end{aligned}\quad (\text{A20})$$

Appendix B: Evolution of the spin population

Using the result of momentum distribution, we can find the change in populations to leading order:

$$\begin{aligned}\delta N_\sigma &= \sum_{\mathbf{p}} n_{p\sigma}^{(2)}(t) \\ &= -\frac{2}{V^2} \sum_{pkqr} \sum_{\sigma\alpha\beta\gamma} Q_{pkqr}^{\sigma\alpha\beta\gamma} g^{(2)}(\sigma, \alpha; \beta, \gamma) F(E_{pkqr}, t).\end{aligned}\quad (\text{B1})$$

Notice that this result does not involve the corrections of $O(U_0^2)$ and $O(U_1 U_0)$ to the momentum distribution. This is because the initial interaction conserves the population of the different spin components.

For intermediate to long times, we notice that, formally,

$$\lim_{t \rightarrow +\infty} F(E, t) \propto t \delta(E) \quad (\text{B3})$$

and therefore the rate of population change of the different components is given by golden-rule expression in Eq. (25). This rate is proportional to the phase-space volume available for scattering with SCCs. We note, this is result is independent of the initial interaction which preserves the $SU(N)$ symmetry.

-
- [1] M. A. Cazalilla, A. F. Ho, and M. Ueda, *New Journal of Physics* **11**, 103033 (2009).
- [2] A. V. Gorshkov, M. Hermele, V. Gurarie, C. Xu, P. S. Julienne, J. Ye, P. Zoller, E. Demler, M. D. Lukin, and A. M. Rey, *Nat Phys* **6**, 289 (2010).
- [3] M. A. Cazalilla and A. M. Rey, *Reports on Progress in Physics* **77**, 124401 (2014).
- [4] R. Yamazaki, S. Taie, S. Sugawa, and Y. Takahashi, *Phys. Rev. Lett.* **105**, 050405 (2010).
- [5] S. Stellmer, R. Grimm, and F. Schreck, *Phys. Rev. A* **84**, 043611 (2011).
- [6] I. Affleck and J. B. Marston, *Phys. Rev. B* **37**, 3774 (1988).
- [7] J. B. Marston and I. Affleck, *Phys. Rev. B* **39**, 11538 (1989).
- [8] P. Coleman, *Phys. Rev. B* **28**, 5255 (1983).
- [9] N. Read and D. M. Newns, *Journal of Physics C: Solid State Physics* **16**, L1055 (1983).
- [10] N. Read and D. Newns, *Adv. Phys.* **36** (1987).
- [11] N. Read and S. Sachdev, *Nucl. Phys. B* **316** (1989).
- [12] C.-H. Cheng and S.-K. Yip, *Phys. Rev. A* **95**, 033619 (2017).
- [13] S. Barbarino, L. Taddia, D. Rossini, L. Mazza, and R. Fazio, *Nat. Commun.* **6** (2015).
- [14] S. Barbarino, L. Taddia, D. Rossini, L. Mazza, and R. Fazio, *New Journal of Physics* **18**, 035010 (2016).
- [15] A. Celi, P. Massignán, J. Ruseckas, N. Goldman, I. B. Spielman, G. Juzeliūnas, and M. Lewenstein, *Phys. Rev. Lett.* **112**, 043001 (2014).
- [16] M. E. Beverland, G. Alagic, M. J. Martin, A. P. Koller, A. M. Rey, and A. V. Gorshkov, *Phys. Rev. A* **93**, 051601 (2016).
- [17] M. Hermele, V. Gurarie, and A. M. Rey, *Phys. Rev. Lett.* **103**, 135301 (2009).
- [18] J. Dufour and F. Mila, *Phys. Rev. A* **94**, 033617 (2016).
- [19] P. Nataf and F. Mila, *Phys. Rev. B* **93**, 155134 (2016).
- [20] S. Sugawa, K. Inaba, S. Taie, R. Yamazaki, M. Yamashita, and Y. Takahashi, *Nature Physics* **7**, 642 EP (2011).
- [21] S. Taie, R. Yamazaki, S. Sugawa, and Y. Takahashi, *Nature Physics* **8**, 825 EP (2012).
- [22] H. Ozawa, S. Taie, Y. Takasu, and Y. Takahashi, *Phys. Rev. Lett.* **121**, 225303 (2018).
- [23] C. Hofrichter, L. Riegger, F. Scazza, M. Höfer, D. R. Fernandes, I. Bloch, and S. Fölling, *Phys. Rev. X* **6**, 021030 (2016).
- [24] X. Zhang, M. Bishof, S. L. Bromley, C. V. Kraus, M. S. Safronova, P. Zoller, A. M. Rey, and J. Ye, *Science* **345**, 1467 (2014), <http://science.sciencemag.org/content/345/6203/1467.full.pdf>.
- [25] G. Cappellini, M. Mancini, G. Pagano, P. Lombardi, L. Livi, M. Siciliani de Cumis, P. Cancio, M. Pizzocaro, D. Calonico, F. Levi, C. Sias, J. Catani, M. Inguscio, and L. Fallani, *Phys. Rev. Lett.* **113**, 120402 (2014).
- [26] F. Scazza, C. Hofrichter, M. Hofer, P. C. De Groot, I. Bloch, and S. Fölling, *Nat Phys* **10**, 779 (2014).
- [27] T. Ozawa and G. Baym, *Phys. Rev. A* **82**, 063615 (2010).
- [28] D. Banerjee, M. Bögli, M. Dalmonte, E. Rico, P. Stebler, U.-J. Wiese, and P. Zoller, *Phys. Rev. Lett.* **110**, 125303 (2013).

- [29] J. Berges, S. Borsányi, and C. Wetterich, *Phys. Rev. Lett.* **93**, 142002 (2004).
- [30] M. Moeckel and S. Kehrein, *Phys. Rev. Lett.* **100**, 175702 (2008).
- [31] M. Moeckel and S. Kehrein, *Annals of Physics* **324**, 2146 (2009).
- [32] N. Nessi, A. Iucci, and M. A. Cazalilla, *Phys. Rev. Lett.* **113**, 210402 (2014).
- [33] S. A. Hamerla and G. S. Uhrig, *Phys. Rev. B* **89**, 104301 (2014).
- [34] M. Eckstein, M. Kollar, and P. Werner, *Phys. Rev. Lett.* **103**, 056403 (2009).
- [35] N. Nessi and A. Iucci, *ArXiv e-prints* (2015), arXiv:1503.02507 [cond-mat.quant-gas].
- [36] M. Marcuzzi, J. Marino, A. Gambassi, and A. Silva, *Phys. Rev. Lett.* **111**, 197203 (2013).
- [37] F. H. L. Essler, S. Kehrein, S. R. Manmana, and N. J. Robinson, *Phys. Rev. B* **89**, 165104 (2014).
- [38] T. Langen, T. Gasenzer, and J. Schmiedmayer, *Journal of Statistical Mechanics: Theory and Experiment* **2016**, 064009 (2016).
- [39] M. Moeckel and S. Kehrein, *New Journal of Physics* **12**, 055016 (2010).
- [40] L. Rademaker, *ArXiv e-prints* (2017), arXiv:1710.09761 [cond-mat.str-el].
- [41] A. Mitra, *Phys. Rev. B* **87**, 205109 (2013).
- [42] M. A. Cazalilla, *Phys. Rev. Lett.* **97**, 156403 (2006).
- [43] M. Buchhold, M. Heyl, and S. Diehl, *Phys. Rev. A* **94**, 013601 (2016).
- [44] Z.-X. Gong and L.-M. Duan, *New Journal of Physics* **15**, 113051 (2013).
- [45] M. Kollar, F. A. Wolf, and M. Eckstein, *Phys. Rev. B* **84**, 054304 (2011).
- [46] M. A. Cazalilla and M.-C. Chung, *Journal of Statistical Mechanics: Theory and Experiment* **2016**, 064004 (2016).
- [47] M. Babadi, E. Demler, and M. Knap, *Phys. Rev. X* **5**, 041005 (2015).
- [48] V. Alba and M. Fagotti, *ArXiv e-prints* (2017), arXiv:1701.05552 [cond-mat.stat-mech].
- [49] ping zou and Z.-M. Zhang, *Journal of Physics B: Atomic, Molecular and Optical Physics* (2018).
- [50] L. Vidmar and M. Rigol, *Journal of Statistical Mechanics: Theory and Experiment* **2016**, 064007 (2016).
- [51] M. Rigol, V. Dunjko, V. Yurovsky, and M. Olshanii, *Phys. Rev. Lett.* **98**, 050405 (2007).
- [52] P. Calabrese, F. H. L. Essler, and M. Fagotti, *Phys. Rev. Lett.* **106**, 227203 (2011).
- [53] E. Ilievski, J. De Nardis, B. Wouters, J.-S. Caux, F. H. L. Essler, and T. Prosen, *Phys. Rev. Lett.* **115**, 157201 (2015).
- [54] T. M. Wright, M. Rigol, M. J. Davis, and K. V. Kheruntsyan, *Phys. Rev. Lett.* **113**, 050601 (2014).
- [55] N. Andrei, *ArXiv e-prints* (2016), arXiv:1606.08911 [cond-mat.quant-gas].
- [56] M. Kormos, M. Collura, and P. Calabrese, *Phys. Rev. A* **89**, 013609 (2014).
- [57] M. Kormos, A. Shashi, Y.-Z. Chou, J.-S. Caux, and A. Imambekov, *Phys. Rev. B* **88**, 205131 (2013).
- [58] M. Rigol, V. Dunjko, and M. Olshanii, *Nature* **452**, 854 EP (2008).
- [59] L. F. Santos and M. Rigol, *Phys. Rev. E* **82**, 031130 (2010).
- [60] L. F. Santos and M. Rigol, *Phys. Rev. E* **81**, 036206 (2010).
- [61] M. Rigol, *Phys. Rev. A* **80**, 053607 (2009).
- [62] M. Rigol, *Phys. Rev. Lett.* **103**, 100403 (2009).
- [63] G. Biroli, C. Kollath, and A. M. Läuchli, *Phys. Rev. Lett.* **105**, 250401 (2010).
- [64] T. Mori, T. N. Ikeda, E. Kaminishi, and M. Ueda, *Journal of Physics B: Atomic, Molecular and Optical Physics* **51**, 112001 (2018).
- [65] K. Mallayya and M. Rigol, *Phys. Rev. Lett.* **120**, 070603 (2018).
- [66] Y. Tang, W. Kao, K.-Y. Li, S. Seo, K. Mallayya, M. Rigol, S. Gopalakrishnan, and B. L. Lev, *Phys. Rev. X* **8**, 021030 (2018).
- [67] M. Eckstein, M. Kollar, and P. Werner, *Phys. Rev. B* **81**, 115131 (2010).
- [68] M. Van Regemortel, H. Kurkjian, I. Carusotto, and M. Wouters, *ArXiv e-prints* (2018), arXiv:1803.07459 [cond-mat.quant-gas].
- [69] R. Barnett, A. Polkovnikov, and M. Vengalattore, *Phys. Rev. A* **84**, 023606 (2011).
- [70] J. G. Cosme, *Phys. Rev. A* **97**, 043610 (2018).
- [71] B. Neyenhuis, J. Smith, A. C. Lee, J. Zhang, P. Richerme, P. W. Hess, Z.-X. Gong, A. V. Gorshkov, and C. Monroe, *ArXiv e-prints* (2016), arXiv:1608.00681 [quant-ph].
- [72] M. Gring, M. Kuhnert, T. Langen, T. Kitagawa, B. Rauer, M. Schreitl, I. Mazets, D. A. Smith, E. Demler, and J. Schmiedmayer, *Science* **337**, 1318 (2012).
- [73] C. Eigen, J. A. P. Glidden, R. Lopes, E. A. Cornell, R. P. Smith, and Z. Hadzibabic, *ArXiv e-prints* (2018), arXiv:1805.09802 [cond-mat.quant-gas].
- [74] M. Stark and M. Kollar, *ArXiv e-prints* (2013), arXiv:1308.1610 [cond-mat.str-el].
- [75] A. Chiocchetta, M. Tavora, A. Gambassi, and A. Mitra, *Phys. Rev. B* **94**, 134311 (2016).
- [76] C.-H. Huang and M. A. Cazalilla, *Phys. Rev. A* **99**, 063612 (2019).
- [77] S.-K. Yip and T.-L. Ho, *Phys. Rev. A* **59**, 4653 (1999).
- [78] S. Blatt, T. L. Nicholson, B. J. Bloom, J. R. Williams, J. W. Thomsen, P. S. Julienne, and J. Ye, *Phys. Rev. Lett.* **107**, 073202 (2011).
- [79] R. Ciuryło, E. Tiesinga, and P. S. Julienne, *Phys. Rev. A* **71**, 030701 (2005).
- [80] K. Enomoto, K. Kasa, M. Kitagawa, and Y. Takahashi, *Phys. Rev. Lett.* **101**, 203201 (2008).
- [81] M. Yan, B. J. DeSalvo, B. Ramachandran, H. Pu, and T. C. Killian, *Phys. Rev. Lett.* **110**, 123201 (2013).
- [82] P. O. Fedichev, Y. Kagan, G. V. Shlyapnikov, and J. T. M. Walraven, *Phys. Rev. Lett.* **77**, 2913 (1996).
- [83] M. Theis, G. Thalhammer, K. Winkler, M. Hellwig, G. Ruff, R. Grimm, and J. H. Denschlag, *Phys. Rev. Lett.* **93**, 123001 (2004).
- [84] R. Yamazaki, S. Taie, S. Sugawa, and Y. Takahashi, *Phys. Rev. Lett.* **105**, 050405 (2010).
- [85] C. Gramsch and M. Potthoff, *Phys. Rev. B* **92**, 235135 (2015).
- [86] N. Tsuji and P. Werner, *Phys. Rev. B* **88**, 165115 (2013), arXiv:1306.0307 [cond-mat.str-el].